remote sensing

MDPI

Article

Specific Effects of the 1988 Earthquake on Topography and Glaciation of the Tsambagarav Ridge (Mongolian Altai) Based on Remote Sensing and Field Data

Anna Agatova [1,2,*], Roman Nepop [1,2], Dmitry Ganyushkin [3], Demberel Otgonbayar [4], Semen Griga [3] and Ivan Ovchinnikov [1]

[1] Institute of Geology and Mineralogy, Siberian Branch of the Russian Academy of Sciences (IGM SB RAS), Koptyuga av., 3, 630090 Novosibirsk, Russia; rnk@igm.nsc.ru (R.N.); c14ovchinnikov@gmail.com (I.O.)
[2] Research Center "Eurasian Integration: History, Politics, Economics", Ural Federal University, Mira Str., 19, 620002 Yekaterinburg, Russia
[3] Institute of Earth Sciences, St. Petersburg State University, Universitetskaya nab., 7–9, 199034 Saint Petersburg, Russia; d.ganyushkin@spbu.ru (D.G.); semyon.griga@yandex.ru (S.G.)
[4] Department of Geography and Geology, Khovd University, Khovd 84153, Mongolia; summit_aamo@mail.ru
* Correspondence: agat@igm.nsc.ru

Abstract: Strong earthquakes could serve as a trigger for glacier detachment and associated ice–rock avalanches. The 1988 Tsambagarav earthquake (M = 6.4) initiated collapse of part of the glacier tongue and a further ice–rock avalanche with an abnormal 5 km long path in Zuslan valley, Tsambagarav ridge (Mongolian Altai). Early documentation of surface effects in 1988, remote sensing and field data gathered 16 and 30 years after this event allowed for the assessment of the seismic impact on a reduction of "damaged" glacier under conditions of global warming as well as estimating topography changes in this arid and seismically active area. Because of the earthquake, the glacier immediately lost 10.4 % of its area (0.1 km^2 of tongue surface). Additionally, 56% of its area was lost during 1988–2015, shrinking much faster than neighboring glaciers of similar size and exposition. Collapse of snow–ice cornice in the accumulation zone could play a key role in rapid acceleration of the detached ice block and abnormally long path of the ice–rock avalanche. A large amount of debris material provided more than 16 years of ice melting. Downstream, the valley avalanche debris cover repeats the topography of underlying Pleistocene moraines, which should be considered in regional paleogeographical reconstructions.

Keywords: Mongolian Altai; Tsambagarav ridge; glaciation; seismicity; 1988 Tsambagarav earthquake; ice–rock avalanche; remote sensing; field research

Citation: Agatova, A.; Nepop, R.; Ganyushkin, D.; Otgonbayar, D.; Griga, S.; Ovchinnikov, I. Specific Effects of the 1988 Earthquake on Topography and Glaciation of the Tsambagarav Ridge (Mongolian Altai) Based on Remote Sensing and Field Data. *Remote Sens.* **2022**, *14*, 917. https://doi.org/10.3390/rs14040917

Academic Editors: Cristiano Tolomei, Sergey V. Popov, Gang Qiao, Xiangbin Cui and Nikola Besic

Received: 26 January 2022
Accepted: 11 February 2022
Published: 14 February 2022

1. Introduction

The modern retreat of glaciers and intensive transformation of alpine landscapes in arid Central Asia, as well as in other high mountain regions, are caused by the ongoing global warming. The retreat of glaciers in the Altai, the northern flank of the Central Asian mountain belt, has been observed since the end of the 19th century and has recently significantly accelerated [1–5]. The last decade was the warmest in the history of meteorological observations since 1891, according to the World Meteorological Organization data. Thus, in Mongolia, the average annual temperature has increased by 2.1 °C since 1940. This has been accompanied by aridity intensification—the annual precipitation has decreased by 7% according to IRIMHE (the Information and Research Institute of Meteorology, Hydrology and Environment of Mongolia) [6]. Such climate changes do not contribute to the preservation of glaciation in the center of the largest continent of the Earth. Thus, within the Mongolian Altai, the area of glaciers—one of the main sources of fresh water in the region—is steadily decreasing [5,7–9].

At the same time, glacier degradation is affected by processes that are not always directly related to the climate. Cataclysmic glacier detachments and associated ice–rock avalanches in the nival–glacial zone led to an almost instantaneous removal of large volumes of ice, snow and debris to lower hypsometric levels [10–12]. Such processes in ice- and snow-rich high mountain environments are very mobile—frictional heating and melting of ice and snow components leads to strongly increased runout distances [13–15]. In the Mongolian Altai, which is characterized by high seismicity, strong earthquakes could serve as a trigger of these events.

The Tsambagarav ridge is the second major center of glaciation in the Mongolian Altai. In tectonic aspect, it represents a front ridge—a large independent tectonic block, separated from the main mountain system by the active Kobdo fault (Figure 1). One of activations of this fault led to the Tsambagarav earthquake (M = 6.4), triggered on 23 July 1988. The main shock, with the epicenter in the Kobdo fault zone, was accompanied by a series of aftershocks. Seismic intensity in the epicenter was VIII points according to the MSK-78 scale.

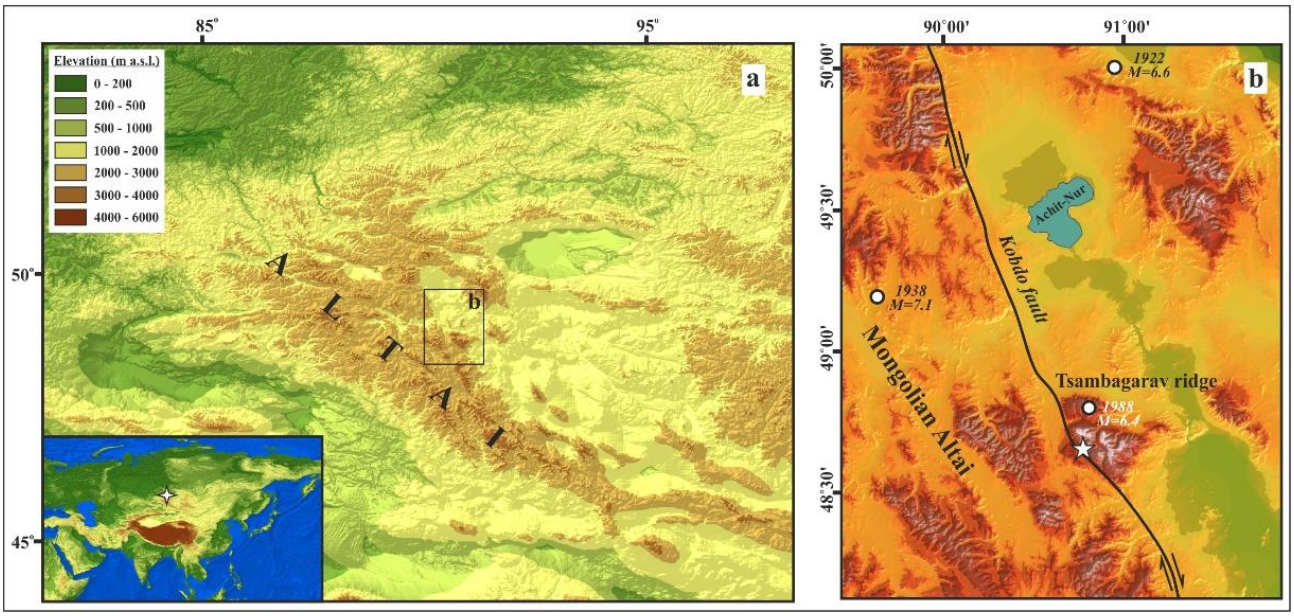

Figure 1. Study area. (**a**) Location of the study area within the Altai mountain system. (**b**) Position of the Zuslan valley (white star) within the Tsambagarav ridge. Circles show epicenters of strong historic earthquakes, year of event and its magnitude.

According to observations immediately after seismic excitation, the maximum ground effects were reported in the high mountain Tsambagarav ridge [16]. The most noticeable among the secondary seismic-gravitational deformations (rockfalls, landslides etc.) was an ice–rock avalanche that ran from the southern slope of the ridge along the Zuslan river valley on 9 August 1988, i.e., 17 days after the main shock. As a result of the earthquake, large cracks of northwestern direction were formed on the surface of one of the glaciers, located in the upper reaches of the Zuslan river basin on the slope of the highest Tsast-Ula summit (4208.4 m a.s.l.). According to [16], a decrease of ice friction on the glacier bed due to intensive melting and the influx of melt water, plastic deformation of ice and aftershock activity, resulted in the loss of stability of a detached ice block of about 6 million m^3 and its further caving into the Zuslan river valley. The triggered ice–rock avalanche traveled about 5 km downstream, striking and jumping from one valley slope to another. The abnormally long path of the avalanche, more than 10 times larger than a typical path calculated for similar conditions [17], allowed the avalanche mechanism to be attributed to the movement on an "air cushion". Total volume of deposited material was estimated to be about 12×10^6 m^3 with an equal ratio of ice and rock components [16].

Thus, as a result of seismic excitation, one of the glaciers in the Tsambagarav ridge simultaneously lost a significant amount of ice, and the Zuslan river valley, for about 5 km, was filled with ice and debris to a height of up to 30 m. Detailed documentation of surface effects immediately after this event [16] provided us with an excellent opportunity to assess the impact of the seismic process on the reduction of mountain glaciation and the topography changes within trough valleys of arid Central Asia. Such an assessment for the Altai uplift was carried out for the first time, and, taking into account its high seismicity, determined the relevance of this study. Additionally, of practical interest is the analysis of factors that controlled the anomalous length of the pathway of the ice–rock avalanche traveling from the nival–glacial zone to the foot of the ridge, where the nomadic seasonal settlements are located.

2. Study Area

The Mongolian Altai is located in the seismically active Central Asian collision belt and is repeatedly affected by strong earthquakes. Only in the 20th century were there more than 60 earthquakes here with a magnitude of $M > 5.5$ and an intensity from VII to XI-XII points according to MSK-64 and MSK-78 scales. Several seismic events were accompanied by large disturbances of the earth's surface, and strong earthquakes with $M > 8$ (Bolnaysk in 1905, Fuyun in 1931 and Gobi–Altai in 1957) induced surface faulting up to several hundred kilometers [18]. Active faults determine the seismic regime of Mongolia [19–21], including areas of the neotectonics uplift in the west of the country—the Mongolian Altai, which is a part of the Altai mountain system, located on the territory of Russia, Mongolia, Kazakhstan and China.

The Altai mountain system is a Cenozoic intracontinental orogen, formed as a distant result of the India–Eurasia collision [22,23]. Formation of the Mongolian Altai began in the late Oligocene–Miocene and occurred in two stages [24]. By the end of the first one, arched uplifts and depressions were separated, and the Mongolian Altai towered over the foothill plains by 1–1.5 km. Intensification of tectonic movements and formation of a modern fault-block structure with the topography dissection up to 3.5–4 km occurred in the Middle Pliocene–Holocene. The process continues to the present, as evidenced by high region seismicity.

Tsambagarav is one of the front ridges of the Mongolian Altai. It is predominantly composed of the Late Devonian and Late Silurian intrusive rocks (granodiorites, granites), which cut through the metamorphic schists of the Upper Cambrian-Lower Ordovician. The Tsambagarav ridge is separated from the main uplift by the active Kobdo regional fault, which is expressed in topography by a narrow rectilinear tectonic depression and by scarp facing the main uplift, and further to the northwest—by a rectilinear scarp facing the Achit-Nur depression (Figure 1). The Tsambagarav ridge has a complicated structure and consists of three adjacent tectonic blocks. These blocks are displaced relative to each other along the faults both horizontally and vertically. In topography, the fault boundaries of the ridge and tectonic blocks in its structure are represented by scarps up to 1 km high, chains of tectonic facets of triangular and trapezoidal shapes, as well as water gaps and rectilinear sections of river valleys (intersections of faults are displayed in topography by sharp, up to 90°, bends of the valleys). Such a knee-like bend there is also at the intersection of the Kobdo fault and Zuslan river valley. Numerous traces of past earthquakes including steep scarps at the base of tectonic facets, seismic cracks displacing Pleistocene moraines, talus fans and watercourses, are observed along the boundaries of tectonic blocks of different ranks (Figure 2).

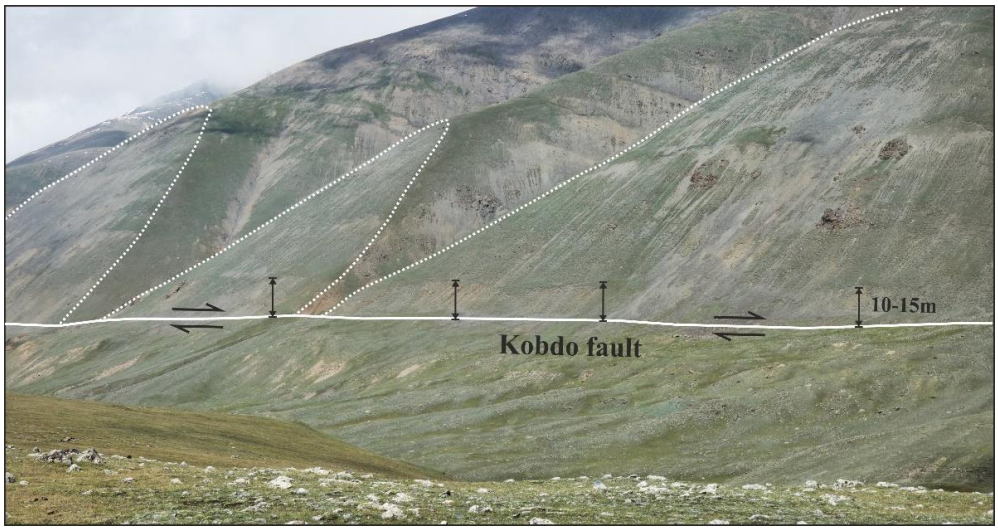

Figure 2. Tectonic facets (dotted line) and seismogenic scarp (vertical lines) at the base of the southwestern slope of the Tsambagarav ridge (photo Agatova).

The largest block in the structure of the Tsambagarav ridge has a triangular (in plan) shape and is the highest one. Its flattened watershed with the main peaks 4208.4 (Tsast-Ula), 4102 and 4025 m a.s.l. rises above the snow line. This determines the widespread distribution of flat-top glaciers here. Their area is about 40% of the total glaciated area [9]. Valley and kar glaciers occupy a position on the periphery of flat-top glaciers, forming glacial complexes. The largest trough valleys with traces of powerful Pleistocene glaciation are cut into this block from the north. The northern slope also hosts the largest contemporary glaciers of the valley, kar valley and hanging types [8,9].

Modern glaciation of the Tsambagarav ridge arose in the middle of the Holocene, about 6 ka ago [25], and is rapidly decreasing at the present time [5,7–9]. Since the maximum of the Little Ice Age, the area of glaciation has decreased by 47%, the equilibrium line has risen by 165 m. Today, it has resulted in the isolation of seven glacial complexes. They include 67 glaciers with a total area of 68.41 km^2 (as of 2015). The weighted average height of the firn line within these glacial complexes is about 3748 m a.s.l. [9]. The largest of the glacial complexes is associated with the Tsast-Ula summit—the highest point of the ridge. On its southern slope in the upper reaches of the Zuslan river, there are predominantly hanging and kar valley glaciers. Among them, the kar glacier No. 15 (according to [9]) is the smallest one. In particular, this glacier was the source of the 1988 ice–rock avalanche and became the object of our research.

Due to its position in the Central part of Eurasia, the climate of the Tsambagarav is characterized by low annual precipitation. Available climatic data refer to the foots of the ranges where the hydrometeorological stations Bayannur (1364 m a.s.l., 35 km to the northeast, measurement period 1995–2004) and Erdenburen (1250 m a.s.l., 35 km to the southeast, measurement period 1962–2002) are located. Average annual air temperature is −5.6 °C, average winter −22.3 °C, average summer 16.5 and 16.6 °C; the average annual precipitation is 87 and 78 mm, respectively, with a predominance of the northwestern direction of moisture transfer [8]. The precipitation at the altitude of the firn boundary is estimated at about 270 mm [26]. Increase in precipitation with altitude, the position of the main watershed above the snow line, the predominance of flattened peaks as well as slope exposition and snowdrift transport are the main factors that determine the glaciation of the Tsambagarav ridge in such arid conditions.

3. Methods

A set of methods, including remote sensing and field research, were used for analyzing the changes of the "damaged" glacier No. 15 since 1988, topography changes in the Zuslan

river valley after passing and melting the ice–rock avalanche, as well as for clarification of the factors that could control the "air cushion" mechanism of the avalanche.

Rates of degradation of glacier No. 15 and neighboring glaciers before and after the 1988 Tsambagarav earthquake were compared based on the analysis of space images for different dates: 11 August 1968 (Corona), 22 June 1988 (Landsat 5), 3 August 1989 (Landsat 5), 14 July 1996 (Landsat 5), 14 July 2002 (Landsat 5), 26 July 2006 (Landsat 5), 15 August 2015 (Landsat 8) and 2 August 2019 (Sentinel-2). Spatial resolution was 1.83 m for Corona images, 10 m—for Sentinel-2, 15 m—for Landsat 8 and 30 m—for Landsat 5. For Landsat 5, Landsat 8 and Sentinel-2 images, a channel combination was applied (543; 543 and 753; 432, respectively). Spatial resolution was improved (Pan-sharpening) for Landsat 8 images. Mapinfo and ArcGIS software were applied for space images interpretation. When interpreting images and carrying out glaciation reconstructing, a mapping area of 0.01 km^2 was used as the minimum area.

To reconstruct the possible mechanism of the ice block detachment, its volume was estimated by applying different approaches. Then, this volume was compared with the volume of the ice component of the avalanche deposits.

The average thickness of the glacier that served a source of ice was calculated applying the regional empirical correlation for Altai kar and kar-hanging glaciers [27]:

$$V = 0.0487F^{1.244}, \quad (1)$$

V—glacier volume; F—glacier area.

The GlabTop model [28] was used to determine the ice thickness in the individual points of the glacier. The magnitude of the shear stress on the bed (τ) was calculated by applying its empirical dependence on the difference in heights ΔH between the highest and lowest points of the glacier [29]:

$$\tau = 0.005 + 1.598\Delta H - 0.435\Delta H^2. \quad (2)$$

The average altitude of the equilibrium line was calculated using the modified Krenke–Khodakov equation [30]. Mass balance was calculated applying the approach based on the air temperature and precipitation data, as well as on the altitude of the firn line [31]. When calculating the ablation, a regional equation was used, obtained as a result of mass balance measurements in the Mongun-Taiga, Turgen-Nuru, and Kharkhira mountain ranges [32]. Applied temperature (0.65 °C/100 m) and annual precipitation (7.7 mm/100 m) gradients were determined for the Tsambagarav ridge [9].

Field research of the Zuslan river valley was carried out twice: in June 2004 and August 2019, 16 years and 31 years after the 1988 Tsambagarav earthquake. Deposits and landforms associated with the ice–rock avalanche were established by interpreting satellite images and by direct studying in the field. To confirm the erosional impact of the avalanche, radiocarbon dating, spore–pollen analysis and estimation of biological composition of peaty soil under avalanche deposits (opened by a pit in 2019) were undertaken. Radiocarbon dating of buried soil was carried out at the Institute of Geology and Mineralogy SB RAS (Novosibirsk). The ^{14}C date was calibrated (2σ standard deviation) by applying the CALIB Rev 7.1 program (http://calib.qub.ac.uk/calib/, accessed on 9 September 2019), with the IntCal13 calibration data set [33]. Spore–pollen analysis was performed by O.B. Kuzmina (A.A. Trofimuk Institute of Petroleum Geology and Geophysics SB RAS, Novosibirsk), determination of biological composition of sediments—by O.N. Uspenskaya (All-Russian Research Institute of Vegetable Growing, Russian Academy of Agricultural Sciences, Vereya).

4. Results

4.1. Shrinkage of Glacier No. 15

Before the 1988 Tsambagarav earthquake, glacier No. 15 was a cirque glacier with a hanging tongue, which was less than one third of the length of the entire glacier. Thus,

this glacier represented a transitional type between the valley and the cirque glaciers. The inclination of the glacier tongue was up to 25° (an average value about 11° according to the SRTM of the year 2000, and about 26° according to the topographic map of scale 1: 100,000, which, despite the small scale, better reflects the state of the glacier at the time of the Tsambagarav earthquake). Based on the analysis of space images on 22 June 1988 and 3 August 1989 (before and after the seismic event, Figure 3), the reduction in the area of glacier No. 15 as a result of the simultaneous loss of a part of the tongue is estimated at approximately 0.1 km^2, or 10.4% (Figure 4).

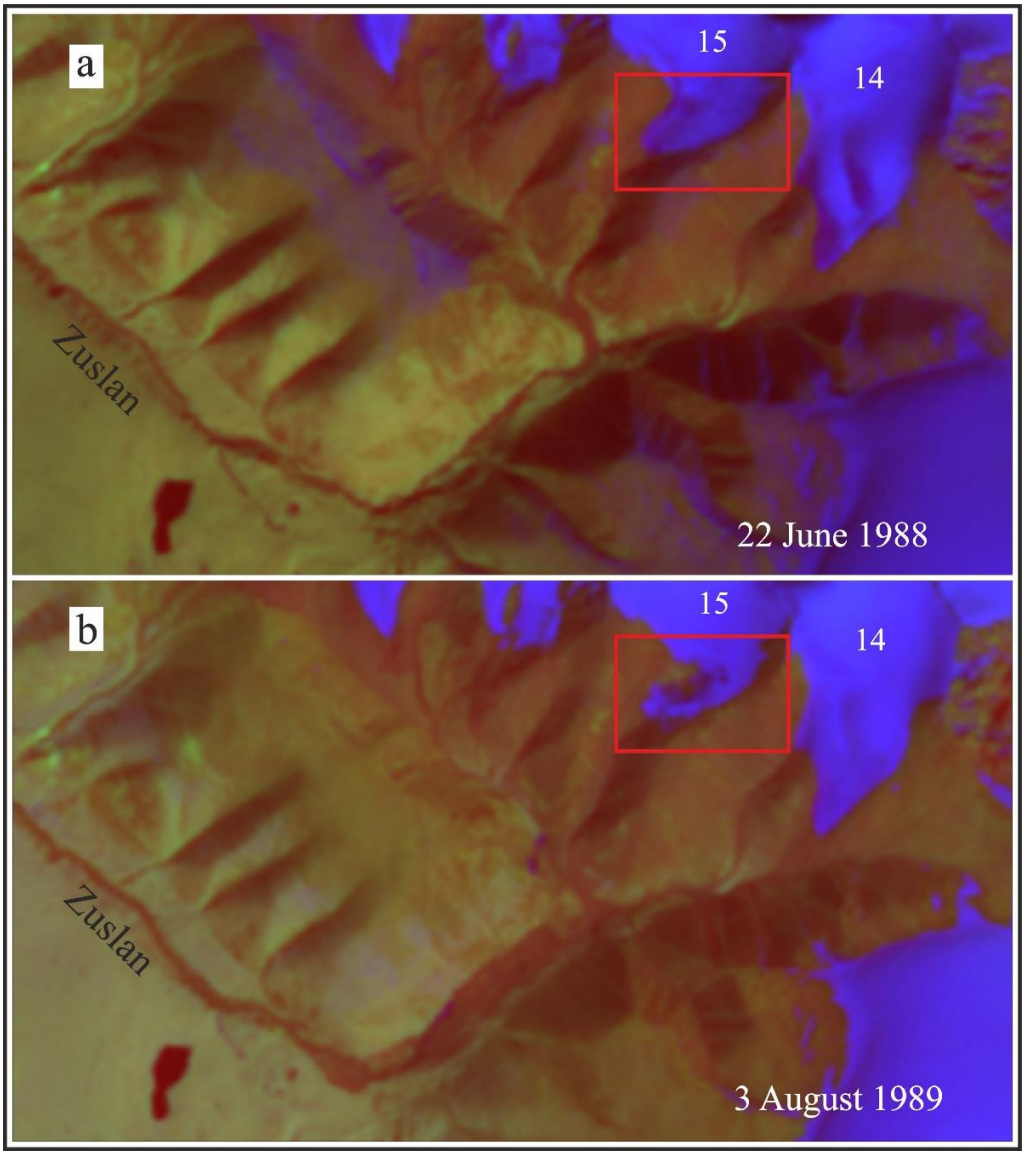

Figure 3. Landsat 5 images showing changes in the area of glacier No. 15 before and after the 1988 Tsambagarava earthquake: (**a**)—22 June 1988, (**b**)—3 August 1989. Red frame outlines the place where changes in glacier area occurred. Note ice-rock avalanche deposits downstream at the bottom of the Zuslan valley (arrows in the panel b).

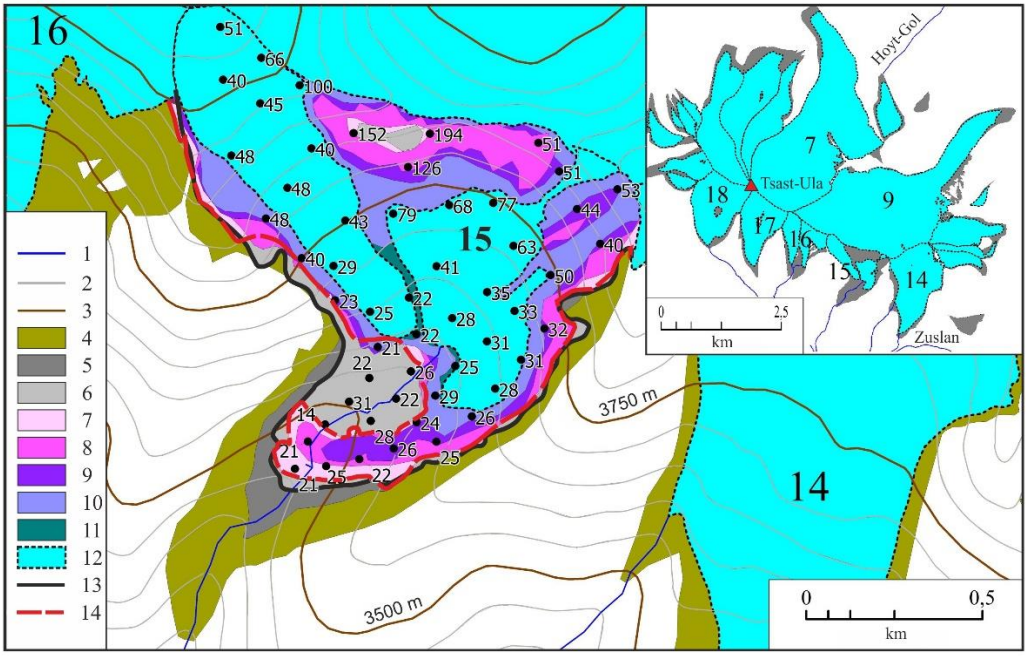

Figure 4. Reduction of glacier No. 15 in the Tsambagarav ridge as a result of the 1988 earthquake according to remote sensing data. 1: rivers (nameless right tributaries of Zuslan river.); 2, 3: elevation lines: 2—every 50 m, 3—every 250 m; 4: glacier at the maximum of the Little Ice Age (LIA); 5–11: areas of glacier reduction based on the results of space imagery interpretation in the periods: 5—from 11 August 1968 to 22 June 1988, 6—from 22 June 1988 to 3 August 1989, 7—from 3 August 1989 to, 14 July 1996, 8—from 14 July 1996 to 14 July 2002, 9—from 14 July 2002 to 26 July 2006, 10—from 26 July 2006 to 15 August 2015, 11—from 15 August 2015 to 2 August 2019; 12: glacier as of 2 August 2019; 13: the boundary of the glacier shortly before the Tsambagarav earthquake (22 June 1988); 14: the boundary of the glacier after the Tsambagarav earthquake (8 March 1989). Dots with numbers indicate glacier thickness (m) according to the GlabTop model. Elevation lines were drawn based on the SRTM 3 digital elevation model (NASA Version 3.0 SRTM Global 1 arc second). The inset shows the reduction of the glacial complex of the Tsast-Ula peak since 1968.

Analysis of satellite images at different times indicates that after the ice block was detached, the glacier bed was exposed in the western part of the tongue. The detached fragment did not completely separate from the glacier tongue (Figure 5a), but already in 1989, the thin bridge in the western edge of the former tongue had melted, while on the eastern periphery, a piece of ice about 100–130 m wide and about 600 m long has been preserved (Figure 4). In its downstream part, it blocked the valley until 2019. For seven years after the earthquake and associated ice–rock avalanche, the glacier area was shrinking mainly due to the melting of this narrow ice fragment. At the same time, most of the glacier was located in the accumulation zone, which led to a short stabilization period of the glacier terminus. However, the glacier did not recover. After 1996, it was intensively retreating (Figures 4 and 5). Since that time, not only has the detached ice block degraded, but the area of outcropping rock protrusions at altitudes of about 3800–3850 m a.s.l. also increased. These processes reflect a rapid decrease in ice thickness.

In 2004, when we visited the Zuslan river valley 16 years after the earthquake, a steep scarp in the glacier body—the detachment wall of the ice block, which initiated the ice–rock avalanche, was still expressed in topography, and the layered structure of ice was clearly visible (Figure 5b). Firn covered the cirque walls, although it had become much thinner than in 1988, while there was no ice or firn on the slope of the southwestern exposure at all. By 2006, the block of ice at the glacier bed had turned into a separated narrow wedge of armored dead ice. Subsequently, a rapid reduction in the area occupied by ice on the cirque

wall continued at altitudes of about 3800 m a.s.l., and by 2015, separation of the glacier into kar and hanging components was outlined.

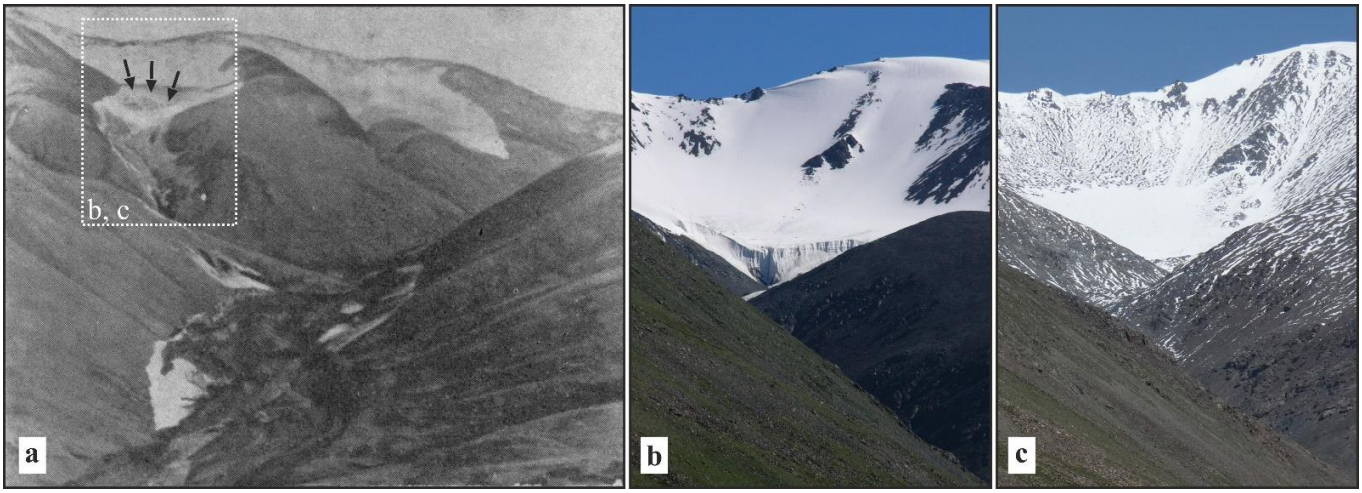

Figure 5. Documentary evidence of the glacier No. 15 reduction as a result of the Tsambagarav earthquake. "Damaged" glacier just after 1988 event (photo Avdeev [16]) (**a**), arrows show the detachment wall of ice block in glacier tongue; (**b**,**c**) views of glacier 16 years (20 July 2004) and 31 years (30 August 2019) after the 1988 seismic event (photo Agatova).

During our visit to the glacier on 2 August 2019, its final separation into two parts (a kar and a hanging one) was detected (Figure 4). The thickness of the glacier had significantly decreased, and rocky protrusions on its bed had been exposed. The scarp (detachment wall) was completely leveled. Firn on the cirque walls was practically absent (Figure 5c). Despite significant decreasing in size, the ice fragment that blocked the valley was still preserved under a debris cover. The water runoff passed under this ice block. Analysis of satellite images at different dates indicates that from 1988 to 2015, when glacier No. 15 lost a fragment of its tongue as a result of the 1988 Tsambagarav earthquake, the area of this glacier decreased by 56%. Over the same period, the area of neighboring glaciers No. 16 and 17 decreased by 35 and 15%, respectively (Figures 4 and 6a). Thus, since the year 1989, i.e., already after the glacier collapse and the reduction of the ablation zone, glacier No. 15 shrank faster than neighboring glaciers: the decreasing of its area in 1989–2015 was 49% compared with 35% and 15% for glaciers No. 16 and 17 respectively.

4.2. Mass Balance of Glacier No. 15 before and after the 1988 Tsambagarav Earthquake

Calculation of mass balance changes are based on the data of the nearest Ulgy meteorological station (1715 m a.s.l., 68 km to the northeast). They were performed for the altitude 3900 m a.s.l.—the position of the equilibrium line at 1988 (before the Tsambagarav earthquake). Mass balance was calculated for the time period 1961–2019 (Figure 6b).

Our calculations indicate that mass balance was stable until 1998 (Figure 6b). After 1998, it experienced an abrupt decrease (more than 500 mm w.e.) and ranged by $-400 \div -600$ mm w.e. It could be stated that under unfavorable climatic conditions, the glacier continued to shrink rapidly (Figure 6a). In 1988, the ratio of the accumulation and ablation areas changed as a result of a sharp reduction of the last one when a part of the glacier tongue was detached. This circumstance, against the background of stable climatic conditions, could seemingly cause a partial restoration of the glacier in the next decade. However, this scenario was not realized and in 1988–1998, the glacier continued to shrink. In 1988, the ablation zone probably decreased in size due to detachment of the tongue fragment. The accumulation zone was also most likely affected by the loss of a significant volume of ice due to the cornice collapse, which occurred without a change in the area of this zone visible in the images.

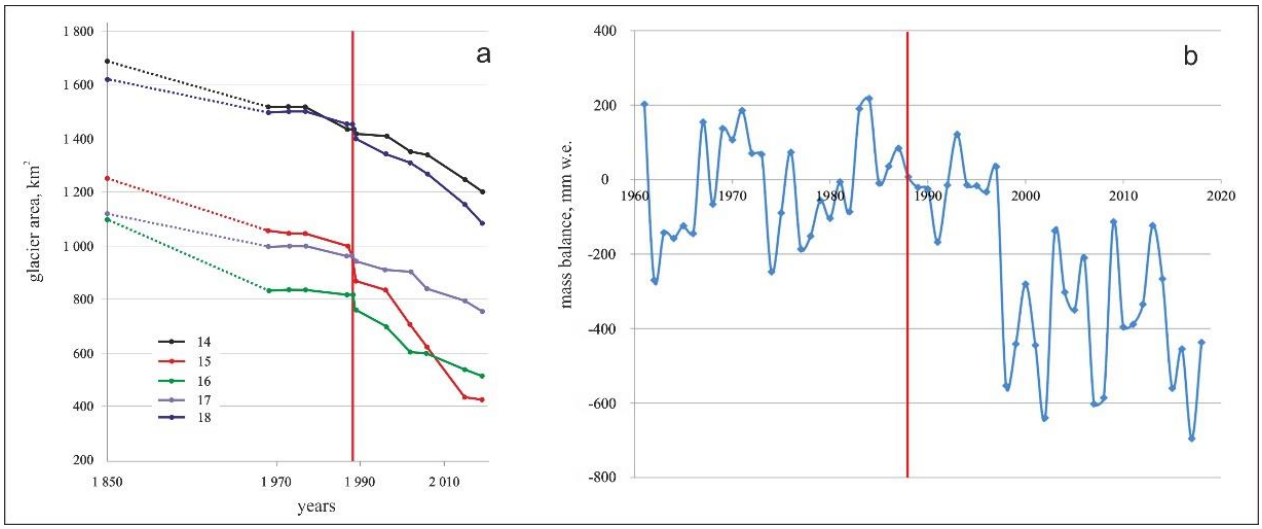

Figure 6. Changes in area of glaciers (No. 14–18) on the south slope of the Tsambagarav ridge and fluctuation of mass balance of glacier No. 15 before and after the 1988 Tsambagarav earthquake. (**a**) Change in the glacier area from the maximum of the Little Ice Age to 2019 according to the interpretation of satellite images; (**b**) fluctuations in the glacier mass balance at the height of the equilibrium line as of 1988 (3900 m a.s.l.) for the period 1961–2019. The red line indicates the 1988 Tsambagarav earthquake.

4.3. Estimation of the Glacier No. 15 Thickness

Estimation of the ice thickness was carried out for different points of the glacier surface by applying the GlabTop model. This model assumes an insignificant effect of the glacier on the underlying bed topography (which corresponds to modern glaciers) and the smoothed character of the latter. All calculations were carried out along the glacier streamlines and then interpolated between these points and the boundaries of the glacier with zero ice thickness. A topographic map of a scale 1:100,000 was used in modeling, because all known DEM for the study area were created later than 1988.

The calculation results are presented in Figure 4. The ice thickness for the glacier part, which was collapsed in 1988, falls within the range of 14–31 m. Ice volume of the glacier as of 22 June 1988, calculated on the basis of empirical relationship for the Altai kar and kar-hanging glaciers [27], is 0.046 km^3, which corresponds to an average ice thickness for the entire glacier of about 48 m.

4.4. Parameters of the Ice–Rock Avalanche

Ice–rock avalanche, triggered by the collapsing of a glacier tongue fragment, started at about 3400 m a.s.l. and traveled 5 km downstream to an altitude of 2840 m a.s.l. (according to Google Earth Pro 7.3.4.8248 software) (Figure 7a,b). Thus, the total height difference is 560 m. It is the largest—about 320 m, on the first kilometer of the path, where the slope inclination reaches 20–25°. This provided a rapid acceleration of the ice–rock breccia. A 70-m high transverse watershed ridge at the end of the first kilometer served as a springboard for the accelerating avalanche. An impact on the slope led to a jump of the ice–rock mass over the ridge. The preservation of the soil cover in the place of jumping over the watershed (Figure 7a,c), as well as the magnitude and length of the splashes, was documented immediately after the avalanche [16]. This is important for understanding the scale and mechanism of this natural phenomenon since the surface effects of an avalanche are rather quickly transformed and erased by subsequent geomorphological processes. The presence of three steep (about 90°) bends in the valley along the path of the avalanche (1, 1.6 and 3.5 km downstream from the place of origin) caused it to be thrown from one slope to another with attenuation of the magnitude of splashes in height from 120 m to 70 and 30 m.

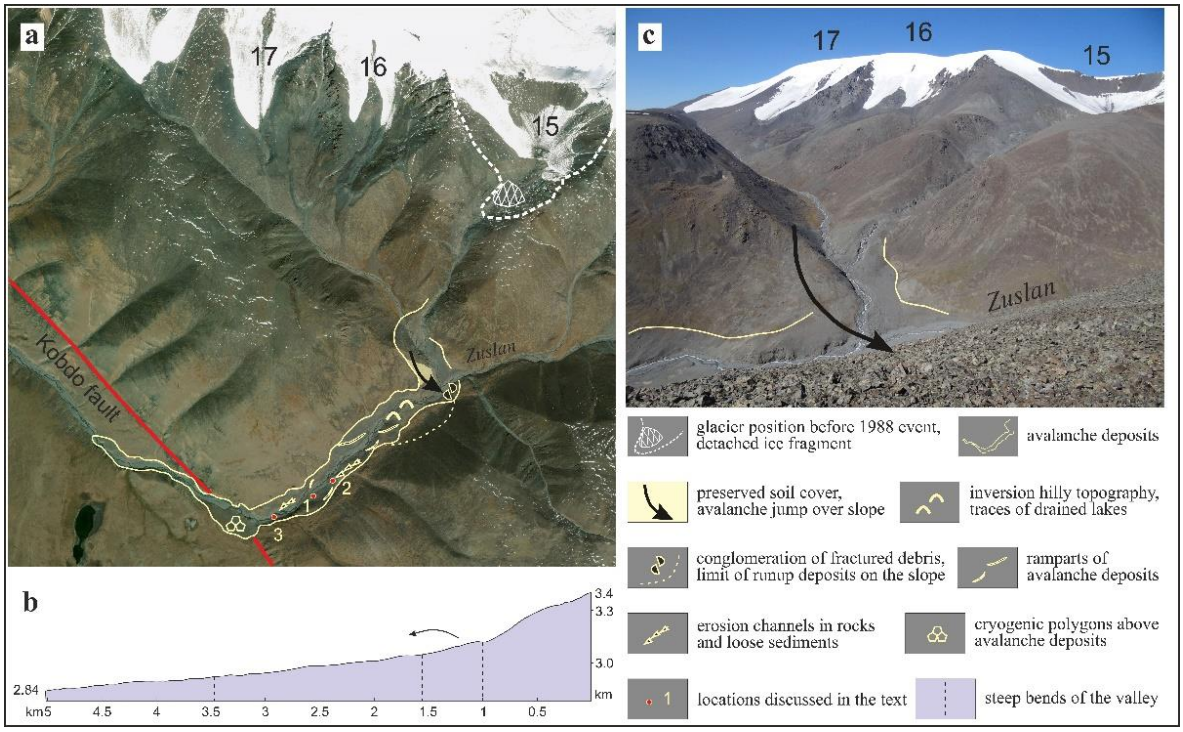

Figure 7. Route of the ice–rock avalanche in the Zuslan valley: (**a**) traces of the ice–rock avalanche in the topography, (**b**) longitudinal profile of the avalanche path and (**c**) view of the upper part of the valley, where ice–rock avalanche jumped over the watershed in the place of the steep (about 90°) bend of the valley. The basis of the scheme is the World-View-2 satellite image; image acquisition date: 19 August 2015. Numbers indicate glaciers discussed in text.

4.5. Changes in the Accumulation Zone of Ice–Rock Avalanches since 1988

In 2004, i.e., 16 years after the avalanche came down, most of the ice in the ice–rock sediments had been already melted, and debris were projected onto the bottom and slopes of the valley. Within the steeper slopes, avalanche deposits were displaced downslope. The river had made a new channel, mainly displaced to the right, more insolated slope of the valley of the southeastern exposure. The channel in many places split into sleeves, bending around the unloaded debris. The basins of temporary lakes formed in 1988 [16] have been already destroyed; fine-grained sediments of these lakes were also projected onto the valley bottom. Nevertheless, in the upper (the northeastern direction) part of the valley, where the avalanche was saturated with ice material to a greater extent, the degradation of buried ice continued on the left bank even in 2004. Ice was exposed under a debris cover along shore benches of the northwestern exposure up to 1–1.5 m high (point 1 in Figures 7 and 8a,b). At the foot of the ice scarps, talus fans accumulated debris material.

It should be emphasized that ramparts, which were formed as a result of ice melting, were clearly expressed in topography and look like lateral moraines. Downstream of the first 90° turn of the valley, in its northwestern-trending part, the debris component of deposits predominated [16]. In 2004, there was no ice in this part of the valley both on the slopes and at the bottom.

Immediately below the sharp turn, removed debris lay on a gentle left slope in the form of a blade about 400 m long and up to 150 m wide. The thin cover of avalanche deposits exactly repeated here the topography of the underlying ancient moraines, but it had a fresher surface—debris were not sodded, were not settled by lichens and many rock fragments had fresh chips and cracks. The debris cover stood out sharply in gray against the background of sodded Pleistocene moraines. In contrast to moraine deposits, represented by large boulders, there are much less large and rounded debris in avalanche

deposits. An increased volume and a fresh appearance of debris cover were noted on the slopes and at the bottom of the erosion gorge in this location.

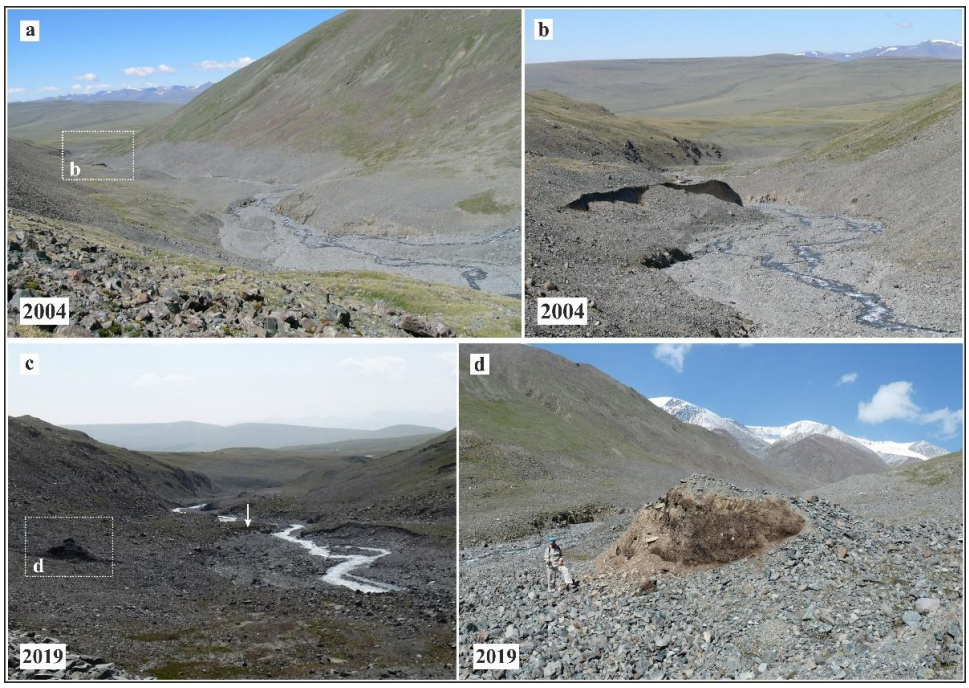

Figure 8. Traces of the 1988 ice–rock avalanche at the bottom of the Zuslan river valley (southwestern oriented part). (**a**,**b**) Scarp on the left bank is formed by buried ice (photo of 2004). View of this part of the valley in 2019: (**c**) arrow shows the same scarp with melted ice; (**d**) peat block 3–4 m high sliding down the slope after ice degradation. Panels (**a**–**c**) view downstream of the valley, and panel (**d**) view upstream of the valley (photo Agatova).

The frontal part of the avalanche, in contrast, did not stand out in the topography, most likely due to the low thickness of sediments projected onto the bottom of the valley and their erosion during seasonal floods. Only a small gray "blotch" of a thin cover of large rounded and non-rounded fragments was discovered on the surface of the right-bank rocky terrace.

In 2019, 31 years after the avalanche came down, on the left-bank section of the valley (where buried ice was exposed in 2004) no one visible outcrop with buried ice was discovered. On the other hand, it could be armored by debris cover and preserved at the foot of the valley slope under newly formed talus cones. At the same time, there were single large (up to 3 × 4 m in area and up to 2–4 m in height) blocks of organo-mineral substrate, probably cut by an avalanche in 1988 (point 2 in Figures 7 and 8c,d). These blocks were placed "on edge" and rotated or turned upside down as a result of ice degradation and intensive sliding in 2004–2019.

A typical landform, indicating the recent filling of the upper part of the valley with ice and rock material, are numerous clusters, often pyramidal, of fragments of various sizes (from boulders to sands and loams), projected onto the bottom of the valley or onto single large boulders as a result of degradation of individual ice blocks. The height of these clusters varies from a few centimeters to 2–3 m. The largest "pyramids" were found at the bottom of the valley in its upper part, where hills up to 5 m high were previously described [16]. Small pyramids, together with fractured debris, often serve as markers of the upper level of avalanche deposits on the valley slopes. A significant amount of broken stones and debris with chips fixed the place of the avalanche impact on the left slope of the Zuslan valley, opposite the mouth of the right tributary, from where it jumped out, already gaining speed (Figure 7). They are concentrated at an altitude of about 30 m above the bottom of the valley (3075 m a.s.l.). We could not confidently identify the

avalanche deposits at a higher altitude in this place, either in 2019 or in 2004, although Avdeev et al. [16] described here ejection of ice–rock sediments in the form of an arc up to 120 m high. Perhaps, due to the low thickness of the deposits, they were dispersed on the surface of the deluvial talus cone. Small swell-like ramparts at the foot of this talus fan may represent the upper level of the run-up sediments (shown in Figure 7). Only a few decades after the event, it is already problematic to take these landforms for avalanche surface effects without information on their initial distribution.

In general, the avalanche deposits are still well recognized on the valley slopes by their bright gray color, but they are sliding noticeably and do not have continuous distribution, as was occurring in 2004. Due to ice melting in the body of the avalanche, the dissection of the topography has decreased. New rocky areas, previously covered with debris, have been exposed. At the same time, the river cut deeper into the sediments projected onto the valley bottom. In some places, distinct floodplain terraces have been already formed.

In the accumulation zone, there are areas where ice–rock avalanche cut off sediments on the slopes and the bottom of the valley. Thus, at the foot of both slopes, the bases of talus and proluvial cones are eroded. In 2019 in the mouth of a large erosional incision on the left valley slope, a ditch was recorded (Figure 7). It represents a marginal channel, that separates avalanche deposits and proluvial cone overlapped by them. Here, small bedrock protrusions smoothed out by an avalanche are also exposed. The same set of erosional landforms was recorded in the rocks downstream the valley on the right riverbank.

Radiocarbon age 1621 ± 201 cal BP (1725 ± 70 SOAN-9838) of a peaty soil horizon is evidence for exaration of the underlying sediments by an avalanche at the valley turn to the northwest (point 3 in Figure 7). This 20-cm thick horizon lies on the left-bank floodplain terrace (2910 m a.s.l.) under a thin (no more than 20 cm in this location) cover of avalanche deposits. The top of the soil profile and/or overlying sediments have been cut away. This conclusion is confirmed by the presence of Botrychium sp. spores in studied peaty soil. This fern grows on moist soils. The results of group biological analysis of bio-residues (>250 microns) also support this conclusion. In addition to the prevailing (90%) herbaceous plants, there are also hygrophilous sedge (Carex) and loosestrife (Lythrum), which do not grow under modern conditions in the valleys of the Tsambagarav ridge.

In 2019, on the surface of the floodplain terrace in this part of the valley, single thermokarst depressions up to 1.5 m in diameter were recorded. They argue for a relatively recent degradation of ice that prevailed in the avalanche body before the turn of the valley.

In the northwest-trending part of the valley, downstream of the sharp turn, cryogenic polygons exhibit on the surface of a thin debris cover on the left gentle river bank (Figure 7). The avalanche deposits have been already settled here by herbaceous vegetation; in some places, a hummock-and-hollow microtopography has formed. In the gorge, cut into the bottom of the valley, projected debris material, predominantly large in size, continues to be unloaded from the slopes (Figure 9).

Figure 9. Ice–rock avalanche deposits above the Pleistocene moraine on the left slope and on the bottom of Zuslan valley at the intersection of the Kobdo fault. People in the middle provide a scale (2019, photo: Agatova). Numbers indicate glaciers discussed in text.

5. Discussion

Glacier detachment was recently recognized as a new type of glacier instability that had been rarely observed and little described [34–36]. The detachment of large parts of alpine glaciers accompanied with ice–rock avalanches are supposed to be not so frequent events. The most well-known among them are the collapses of the Kolka Glacier in the Russian Caucasus and two neighboring glaciers in Tibet's Aru region. At the same time, recent studies suggest more frequent occurrence and effects on topography of these events [11,15]. Glacier detachments often lead to ice–rock avalanches, but on the contrary, ice–rock avalanches are usually triggered by various slope processes and their combinations [10]. A chain of processes initiated by the 1988 Tsambagarav earthquake, finally triggered an ice–rock avalanche in the Zuslan valley (Mongolian Altai). This event instantly affected the topography and caused irreversible changes in glaciation of the Tsambagarav ridge.

5.1. Retreating Rate of Glacier No. 15 in Comparison with Neighboring Glaciers in the Upper Part of the Zuslan River Basin

Comparison of the type, slope exposition, hypsometric position and inclination of glaciers on the southern slope of the Tsast-Ula peak on 22 June 1988, i.e., just before the seismic event, indicates that all glaciers had similar parameters (Table 1, Figure 10). Glacier No. 15 differed from others in more complex structure, i.e., presence of a well-pronounced kar, where a hanging tongue originated. At that time, glacier No. 15 was located even slightly lower than hanging glaciers No. 16–18. Thus, comparison with very similar neighboring glaciers gives an opportunity to analyze the effect of the seismically triggered loss of a tongue fragment on the retreating rate of the damaged glacier under the conditions of ongoing climate warming.

Table 1. Hypsometric parameters of glaciers on the southern slope of the Tsast-Ula peak, Tsambagarav ridge *.

Glacier Number after [9]	Length, km	Lower Point, m a.s.l.	Upper Point, m a.s.l.	Average Altitude, m a.s.l.	Mode, m a.s.l.	Average Inclination, Degree	Slope Exposition (South), Degree
14	1.693	3412	4068	3768	3846	22	191
15	0.974	3445	4090	3750	3649	26	192
16	0.855	3514	4158	3850	4073	28	190
17	1.019	3464	4191	3870	4105	26	190

* SRTM digital elevation model and glacier contours of 22 June 1988 were used for measurements.

Collapse of the glacier tongue fragment of 0.1 km^2 (10.4% of the total area) on 9 August 1988 as a result of the Tsambagarav earthquake strongly affected the glacier No. 15 shrinking. The analysis of satellite images showed that from 1988 to 2015, its area decreased by 56% (Figures 4 and 6), while neighboring glaciers No. 16 and 17 (similar in size, altitude and slope exposition, Table 1), decreased not so significantly, by 35 and 15%, respectively.

Note that under the conditions of progressive climate warming, an abrupt reduction of the ablation zone as a result of the simultaneous loss of several million cubic meters of ice, did not lead to glacier restoration. Even presence of a deep kar, which traditionally serves as an advantage for the preservation of the glacier, contributing to its shading and increased snow concentration, did not become a decisive factor for recovery. After a short stabilization, which lasted until 1997 (Figure 4), the affected glacier shrank, much more rapidly in comparison to neighboring ones. Initially, after the final melting of the tongue, it became a kar glacier, and by the time of our visit in 2019, it had already split into two separate glaciers inside the kar.

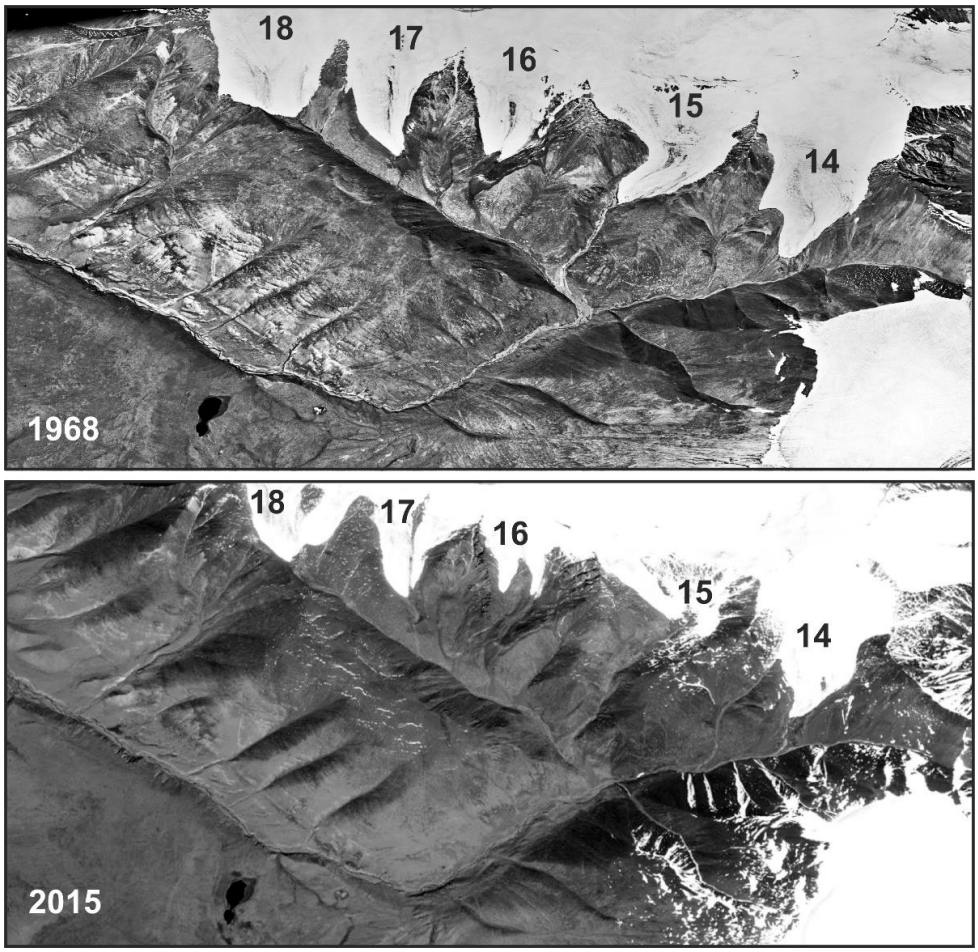

Figure 10. Satellite images of Corona (11 August 1968) and WV02 (19 August 2015) demonstrate the difference in the retreating rate of "damaged" glacier No. 15 in comparison with neighboring glaciers and topography changes of the Zuslan valley after ice–rock avalanche.

5.2. The Probable Mechanism of Ice–Rock Avalanche on an "Air Cushion"

According to [16], during the 1988 Tsambagarav earthquake, the block of ice in the tongue part of the glacier detached from the main body and displaced by several meters in the southeast direction. Melt water ran into the crack and decreased the friction with the glacier bed. Along with plastic deformations of ice and aftershock activity, it caused the movement of the block that triggered an ice–rock avalanche 17 days later. Kääb et al. [11] emphasize the importance of the existing fracturing that controlled the configuration of the detached ice block. One of the cracks in the glacier body actually served as a detachment wall.

According to [11], the formation of a system of cracks—two larger transverse ones and a series of concentric ones, outlining a central depression with a diameter of about 150 m, most likely is associated with the concentration of under-ice meltwater runoff. We believe such fracturing reflects the complicated topography of the glacial bed. In fact, glacier No. 15 has the deepest kar among all neighboring glaciers. Described cracks were actually bergschrunds. Such bergschrunds were practically not expressed on neighboring hanging glaciers (No. 16–18) with a simpler bed geometry and to some extent, were expressed on kar valley glacier No. 14 (Figure 10 upper panel). Generally, the presence of a system of cracks undoubtedly predetermined the separation of the ice block in 1988 precisely in the weakened part of the glacier. The higher dynamic of the glacier No. 15 (expressed in lower position of its tongue in comparison with neighboring glaciers), and the irregular movement of ice (which was a result of more complicated bed topography), may explain why this particular glacier reacted to the seismic shocks.

The affected glacier was shrinking faster than the neighboring ones, even if 1989, rather than 1988, was used as the beginning of the observation period. Even when not considering the glacier collapse, its area decreased by 49%, while the reduction of glaciers No. 16 and 17 was the same (as in the period 1988–2015) 35 and 15%. This became possible despite the fact that the main part of glacier No. 15, which was shrinking after 1989, was located in the altitude range corresponding to the accumulation zone of neighboring glaciers. It was also located in deep kar with larger shaded area. This paradox suggests that the destructive effect of seismic activation was not limited only by collapse of a tongue fragment. Significant losses of the snow–ice mass could also occur in the accumulation zone—in the ridge part of the kar, which caused further rapid exposure of the glacier bed.

This scenario is also evidenced by calculations of the thickness of the detached ice block, which triggered an ice–rock avalanche on 9 August 1988. Avdeev et al. [16] estimated the volume of this block at 6 million m^3. The area of the block, according to our analysis of satellite images from 22 June 1988 and 3 August 1989, was about 0.1 km^2. It allows to calculate average thickness—about 60 m. This is much more than 14–31 m—the thickness of the ice in the glacier tongue, calculated by applying the GlabTop model (Figure 4).

The average ice thickness for the entire glacier as of May 1988, calculated by applying an empirical relationship for the Altai cirque and cirque-hanging glaciers [27], was about 48 m. However, the ice thickness on the tongue may differ from the average value for the whole glacier. Glacier No. 15, as already emphasized, has a well-expressed kar. Due to the centripetal movement of ice and its concentration on the flattened bottom of the kar, the ice thickness within the kar before the earthquake was higher than in the tongue, which occupied a steep (up to 25°) slope. Thus, in this case, too, we can say that volume of the detached ice block (6 million m^3 [16]) is most likely overestimated.

At the same time, estimating the total volume of the avalanche at 12 million m^3 immediately after the earthquake, the researchers noted an equal ratio of ice and rock material [16]. It means that the volume of disintegrated ice was no less than the same 6 million m^3. During the avalanche movement, the rapid disintegration of the detached ice block and associated increase in the volume of ice occurred, as well as partial loss of the volume due to melting as a result of heating under the friction. Taking into account the established deficit of ice in the detached part of the glacier tongue, it can be assumed that missing ice volume could enter the glacier surface, and then into the valley after the collapse of the snow–ice cornice within the accumulation zone.

Probably, on 9 August 1988, this snow–ice cornice collapsed from heights of about 3850–3900 m a.s.l. It hit the already chipped off part of the glacier tongue at an altitude of about 3500–3600 m a.s.l. This event, possibly caused by one of the aftershocks, along with the intensive meltwater influx onto the glacier bed, served as a trigger for the final detaching of the chipped ice block. The resulting impulse explains the rapid acceleration and further jumping of the ice–rock mass over the 70-m high watershed ridge already at the beginning of the path. It also provides a high speed and anomalous way covered by the avalanche, which allowed to assume the air cushion mechanism of its movement [16].

The barely fast and distant (about 5 km) advance of the ice–rock breccia could have been initiated only by the sliding of a tongue fragment, even if considering the greatest steepness of the slope (up to 20–25°) and the height difference (320 m) at the first kilometer of the avalanche path. Additional ice volume, which came from the accumulation zone, also explains the previously noted discrepancy between the volume of ice in the avalanche and the volume of the detached block. The high rate of ice degradation within the accumulation zone of the glacier No. 15 after passing the avalanche is another strong argument in favor of the proposed initiation mechanism. This scenario is indirectly confirmed by the information of a casual observer who was at a considerable distance from the event: "... The moment the avalanche began to move at 18:00 local time, he saw a white cloud rising up in the glacier, and then a rumble came" [16].

The block of ice in the eastern part of the kar bottom of the glacier No. 15 was recorded in the images after the 1988 Tsambagarav earthquake and was preserved until our visit in

2019. It can be an in situ part of the glacial tongue, which was frozen to the bed. However, taking into account the suggested mechanism of avalanche initiation, it is more likely a preserved rear part of the detached tongue fragment, which, during the movement, stopped while it contacted with rocky protrusions in the southeastern part of the valley.

The watershed ridge exerted an additional influence on the acceleration of the ice–rock breccia at the beginning of the path. It actually served as a 70-m springboard. The subsequent run up onto the opposite slope of the Zuslan river valley was the maximum in height (about 120 m). Particularly at this moment, the formation of an air cushion could occur. Such cases have been repeatedly described by eyewitnesses in various seismically active mountain regions of the world [37], and also reconstructed in the framework of studying the Pleistocene and Holocene seismically induced landslides in Altai [38,39]. The possible existence of air "lubrication" during the movement of the avalanche can be indicated by the fact that after the ice degradation and debris projection, the former topography of the valley bottom, nevertheless, was quite recognizable.

5.3. The Rate of Ice Melting and New Landforms Formation in the Avalanche Accumulation Zone over the Past 30 Years

As noted by Avdeev and colleagues [16], the distribution of displaced material in the Zuslan river valley shortly after the event was irregular both in terms of substantial and granulometric composition. In the upper part of the valley, the ice and snow components prevailed, in the lower part—the clastic component. The avalanche created various randomly distributed landforms. Already during the first visit of the site in 1988 [16], there were depressions of drained lakes filled with fine soil along the talweg. Positive landforms were represented by linear ridges, similar to lateral and bottom moraines, and by individual hummocks up to 5–8 m. The thickness of ice–rock deposits in the upper part of the valley was then about 20–25 m; in the middle part of the valley it increased up to 30 m and then gradually decreased downstream the valley.

Observations in 2004 and 2019 showed that the melting of the main volume of ice and the projection of the rocky sediments occurred before 2004; however, even 16 years after the event, buried ice was partially preserved in the upper part of the valley, completely degrading by 2019. Long duration of ice melting outside the nival–glacial zone was controlled by the high content (about half of the volume) of rock debris in the avalanche deposits—the ice was tightly armored. For comparison, according to our field observations in another mountain system of Central Asia, ice melting in the avalanche deposits in the Indian Himalayas occurred in the first years, i.e., an order of magnitude faster. This avalanche was triggered in the upper part of the Teesta river basin by the Sikkim earthquake (M = 6.9) on 18 September 2011. The avalanche was smaller and contained minor amounts of rock debris. During our observation in February 2012, it had not yet started to melt, but already in the 23 October 2013 satellite images (Google Earth database), only the cut lower parts of the slopes and a thin debris cover at the place of its stop indicated the recent path of the avalanche (Figure 11).

In the Tsambagarav ridge, after ice melting in the avalanche deposits, ground effects of this event begin to vanish relatively fast. Already after 30 years, even in the arid climate of Mongolia, the debris cover is being settled by herbal vegetation, its sliding down the slopes become noticeable, the height and clarity of positive landforms (ramparts, hummocks) decrease, and a floodplain terrace is formed. The relatively high rate of leveling the ground effects of the avalanche and the difficulties of their subsequent identification in the topography suggest a greater number of such events, including those of a seismic origin, in the recent geological past than can be established now in the Altai.

In our research carried out in 2004 and 2019, i.e., after the melting of most of the ice in the avalanche deposits, we, like Avdeev and colleagues [16], reported the similarity of new positive linear landforms with areas of hummocky depression in the microtopography of moraines. At the foot of the Tsambagarav ridge, debris carried out by an avalanche along the Zuslan river valley, repeated the topography of the underlying Pleistocene moraines.

This creates the illusion of morphologically fresh moraines, which were relatively recently formed by glaciers advancing from the upper part of the valley. Without knowledge about avalanches, such convergence can complicate the correlation of moraine complexes in different valleys of the ridge, as well as the reconstruction of the number, chronology and magnitude of glacial events in avalanche-hazardous areas. Information about such extended seismically triggered avalanches should be taken into account in paleoglaciological reconstructions.

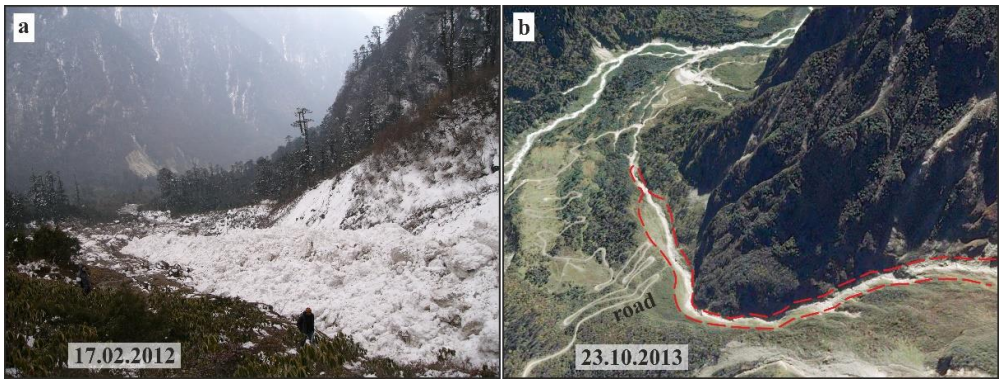

Figure 11. Ice-snow avalanche in the Indian Himalayas, triggered by the Sikkim earthquake on 18 September 2011 ((**a**)—photo Agatova). Its rapid melting ((**b**)—satellite image from the Google Earth database, 23 October 2013) was caused by minor presence of debris component in the avalanche.

6. Conclusions

The results of remote sensing observations and field studies carried out in 2004 and 2019 in the Zuslan river valley of the Tsambagarav ridge made it possible to reach several conclusions.

1. A glacier that lost a significant volume of ice and 10% of area as a result of the 1988 Tsambagarav earthquake and associated ice–rock avalanche, degraded much faster than neighboring glaciers of similar size on the slope of the same exposition. From 1988 to 2015, its area decreased by 56%. It became the only kar glacier among all neighboring hanging glaciers, and by 2019 it had already split into two separate glaciers inside the kar.
2. A key role in the rapid acceleration of the detached ice block could be played by the influx of additional mass as a result of the collapse of the snow–ice cornice in the accumulation zone. This scenario is confirmed by the anomalous length of the avalanche path, the rapid degradation of ice in the accumulation zone and the established ice deficit in the detached part of the glacier tongue in comparison with the initial estimates [16].
3. Under climatic conditions of the Mongolian Altai, the ice melting in the body of an ice–rock avalanche outside the nival–glacial zone occurred mainly in the first 10–15 years after the event (by 2004). Ice completely melted 30 years later (by 2019 or a bit earlier). Such long duration is explained by the high content of debris material—about half of the volume.
4. Deposits and landforms resulting from the ice melting in avalanche deposits resemble glacial deposits and landforms. Debris cover in the lower part of the valley completely repeats the topography of underlying moraines, which, if ignorant with their avalanche origin, can lead to an incorrect interpretation of the age of glacial events in the Tsambagarav ridge.
5. The 1988 Tsambagarav earthquake demonstrated the real possibility of a cataclysmic input of a large volume of ice–rock material from the upper nival–glacial zone to the foot of the Altai high-mountain ranges. It should be taken into account in planning of current economic activities. The rapid erasing of avalanche surface effects by subsequent geomorphological processes suggests that large avalanches, including

those of a seismic origin, took place in the Altai more often than it can now be established in the topography.

Author Contributions: A.A., field geological and geomorphological research, analysis of results, supervision and general leadership; R.N., field geological and geomorphological research and interpretation of space images; D.G., field glaciological research and data curation; D.O., field geomorphological research, data review and editing; S.G., remote sensing data analysis; I.O., radiocarbon dating, data review and editing. All authors have read and agreed to the published version of the manuscript.

Funding: The study was supported by State Assignment of IGM SB RAS and partly funded by Russian Science Foundation (grant 22-27-00447).

Informed Consent Statement: Not applicable.

Acknowledgments: Uspenskaya (All-Russian Research Institute of Vegetable Growing, Russian Academy of Agricultural Sciences, Vereya) is kindly thanked for establishing the biological composition of sediments, and Kuzmina (A.A. Trofimuk Institute of Petroleum Geology and Geophysics SB RAS, Novosibirsk) for providing pollen analysis. We appreciate valuable comments of three anonymous reviewers that helped to improve style and content of the manuscript.

Conflicts of Interest: The authors declare no conflict of interest.

References

1. Shahgedanova, M.; Nosenko, G.; Khromova, T.; Muraveyev, A. Glacier shrinkage and climatic change in the Russian Altai from the mid-20th century: An assessment using remote sensing and PRECIS regional climate model. *J. Geophys. Res. Atmos.* **2010**, *115*, D16107. [CrossRef]
2. Narozhniy, Y.; Zemtsov, V. Current state of the Altai glaciers (Russia) and trends over the period of instrumental observations 1952–2008. *Ambio* **2011**, *40*, 575–588. [CrossRef] [PubMed]
3. Kotlyakov, V.M.; Chernova, L.P.; Zverkova, N.M.; Khromova, T.E. The one-and-a-half-century reduction of Altai glaciers in Russia and Kazakhstan. *Earth Sci.* **2014**, *458*, 1307. [CrossRef]
4. Wei, J.F.; Liu, S.Y.; Xu, J.L.; Guo, W.Q.; Bao, W.J.; Shangguan, D.H.; Jiang, Z.L. Mass loss from glaciers in the Chinese Altai Mountains between 1959 and 2008 revealed based on historical maps, SRTM, and ASTER images. *J. Mt. Sci.* **2015**, *12*, 330–343. [CrossRef]
5. Pan, C.G.; Pope, A.; Kamp, U.; Dashtseren, A.; Walther, M.; Syromyatina, M.V. Glacier recession in the Altai Mountains of Mongolia in 1990–2016. *Geogr. Ann. Ser. A Phys. Geogr.* **2018**, *100*, 185–203. [CrossRef]
6. Vandandorj, S.; Munkhjargal, E.; Boldgiv, B.; Gantsetseg, B. Changes in event number and duration of rain types over Mongolia from 1981 to 2014. *Environ. Earth Sci.* **2017**, *76*, 70. [CrossRef]
7. Kadota, T.; Gombo, D. Recent glacier variations in Mongolia. *Ann. Glaciol.* **2007**, *46*, 185–188.
8. Otgonbayar, D. *Modern Glaciation of the Mongolian Altai (by the Example of the Munhkhairkhan and Sutai Ranges, the Tsambagarav Mountain Knot)*; Business Connect: Barnaul, Russia, 2013; 156p. (In Russian)
9. Ganyushkin, D.A.; Otgonbayar, D.; Chistyakovm, K.V.; Kunaeva, E.P.; Volkov, I.V. Recent glacierization of the Tsambagarav ridge (North-Western Mongolia) and its changes since the Little Ice Age maximum. *Ice Snow.* **2016**, *4*, 437–452. (In Russian) [CrossRef]
10. Schneider, D.; Huggel, C.; Haeberli, W.; Kaitna, R. Unraveling driving factors for large rock–ice avalanche mobility. *Earth Surf. Process. Landf.* **2011**, *36*, 1948–1966. [CrossRef]
11. Kääb, A.; Jacquemart, M.; Gilbert, A.; Leinss, S.; Girod, L.; Huggel, C.; Falaschi, D.; Ugalde, F.; Petrakov, D.; Chernomorets, S.; et al. Sudden large-volume detachments of low-angle mountain glaciers–more frequent than thought. *Cryosphere* **2021**, *15*, 1751–1785. [CrossRef]
12. Shugar, D.H.; Jacquemart, M.; Shean, D.; Bhushan, S.; Upadhyay, K.; Sattar, A.; Westoby, M.J. A massive rock and ice avalanche caused the 2021 disaster at Chamoli, Indian Himalaya. *Science* **2021**, *373*, 300–306. [CrossRef] [PubMed]
13. Petrakov, D.A.; Chernomorets, S.S.; Evans, S.G.; Tutubalina, O.V. Catastrophic glacial multi-phase mass movements: A special type of glacial hazard. *Adv. Geosci.* **2008**, *14*, 211–218. [CrossRef]
14. Huggel, C.; Zgraggen-Oswald, S.; Haeberli, W.; Kääb, A.; Polkvoj, A.; Galushkin, I.; Evans, S.G. The 2002 rock/ice avalanche at Kolka/Karmadon, Russian Caucasus: Assessment of extraordinary avalanche formation and mobility, and application of Quick-Bird satellite imagery. *Nat. Hazards Earth Syst. Sci.* **2005**, *5*, 173–187. [CrossRef]
15. Evans, S.G.; Delaney, K.B. Catastrophic mass flows in the mountain glacial environment. In *Snow and Ice-Related Hazards, Risks, and Disasters*; Hazards and Disasters Series; Haeberli, W., Whitemann, C., Eds.; Elsevier: Amsterdam, The Netherlands, 2015; pp. 563–606.
16. Avdeev, V.A.; Nartov, S.V.; Balzhinnyam, I.; Monhoo, D.; Erdenbileg, B. Tsambagarav earthquake July 23, 1988 (Western Mongolia). *Russ. Geol. Geophys.* **1989**, *11*, 118–124. (In Russian)

17. Scheidegger, A.E. *Physical Aspects of Natural Catastrophes*; Elsevier: New York, NY, USA, 1975; 289p.
18. Khilko, S.D.; Kurushin, R.A.; Kochetkov, V.M.; Misharina, L.A.; Melnikova, V.I.; Gileva, N.A.; Lastochkin, S.V.; Balzhinnyam, I.; Monhoo, D. Earthquakes and the Fundamentals of Seismic Zoning of Mongolia. In *Joint Soviet-Mongolian Research Geological Expedition*; Is. 41; Nauka: Moscow, Russia, 1985; 224p. (In Russian)
19. Tapponnier, P.; Molnar, P. Active faulting and Cenozoic tectonics of the Tien Shan, Mongolia, and Baykal regions. *J. Geophys. Res. Solid Earth* **1979**, *84*, 3425–3459. [CrossRef]
20. Baljinnyam, I.; Bayasgalan, A.; Borisov, B.A.; Cisternas, A.; Dem'yanovich, M.G.; Ganbaatar, L.; Kochetkov, V.M.; Kurushin, R.A.; Molnar, P.; Philip, H.; et al. Ruptures of major earthquakes and active deformation in Mongolia and its surroundings. *Gcol. Soc. Am. Mem.* **1993**, *181*, 62.
21. Demianovich, M.G.; Kljuchevskiy, A.V.; Demianovich, V.M. The main faults of Mongolia and their role in the seismic zoning of the territory. *Lithosphere* **2008**, *3*, 3–13. (In Russian)
22. Molnar, P.; Tapponnier, P. Cenozoic tectonics of Asia: Effects of a continental collision. *Science* **1975**, *189*, 419–426. [CrossRef]
23. Dobretsov, N.L.; Buslov, M.M.; Delvaux, D.; Berzin, N.A.; Ermikov, V.D. Meso- and Cenozoic tectonics of the Central Asian mountain belt: Effects of lithospheric plate interaction and mantle plumes. *Int. Geol. Rev.* **1996**, *38*, 430–466. [CrossRef]
24. Devyatkin, E.V. *Cenozoic of Inner Asia*; Nauka: Moscow, Russia, 1981; 196p. (In Russian)
25. Herren, P.A.; Eichler, A.; Machguth, H.; Papina, T.; Tobler, L.; Zapf, A.; Schwikowski, M. The onset of Neoglaciation 6000 years ago in western Mongolia revealed by an ice core from the Tsambagarav mountain range. *Quat. Sci. Rev.* **2013**, *69*, 59–68. [CrossRef]
26. Bantcev, D.V.; Ganyushkin, D.A.; Chistyakov, K.V.; Volkov, I.V.; Ekaykin, A.A.; Veres, A.N.; Tokarev, I.V.; Shtykova, N.B.; Andreeva, T.A. The Components of the Glacial Runoff of the Tsambagarav Massif from Stable Water Isotope Data. *Geosciences* **2019**, *9*, 297. [CrossRef]
27. Nikitin, S.A. Regularities in the distribution of glacial ice in the Russian Altai, assessment of reserves and dynamics. *Mater. Glaciol. Investig.* **2009**, *107*, 87–96. (In Russian)
28. Paul, F.; Linsbauer, A. Modeling of glacier bed topography from glacier outlines, central branch lines and a DEM. *Int. J. Geogr. Inf. Sci.* **2012**, *26*, 1173–1190. [CrossRef]
29. Haeberli, W.; Hölzle, M. Application of inventory data for estimating characteristics of and regional climate-change effects on mountain glaciers: A pilot study with the European Alps. *Ann. Glaciol.* **1995**, *21*, 206–212. [CrossRef]
30. Koreisha, M.M. *Glaciation of the Verkhoyansk-Kolyma Region*; Russian Academy of Sciences: Moscow, Russia, 1991; 144p. (In Russian)
31. Glazyrin, G.E. *Distribution and Regime of Mountain Glaciers*; Gidrometeoizdat: Leningrad, Russia, 1985; 181p. (In Russian)
32. Ganyushkin, D.A. Wurm and Holocene Evolution of Climate and Glaciation of the Mongun-Taiga Massif (Southwestern Tuva). Ph.D. Thesis, Sant-Petersburg State University, Sant-Petersburg, Russia, 2001; 195p. (In Russian)
33. Reimer, P.J.; Bard, E.; Bayliss, A.; Beck, J.W.; Blackwell, P.G.; Bronk Ramsey, C.; Buck, C.E.; Cheng, H.; Edwards, R.L.; Friedrich, M.; et al. IntCal13 and MARINE13 radiocarbon age calibration curves 0–50000 years cal BP. *Radiocarbon* **2013**, *55*, 1869–1887. [CrossRef]
34. Tian, L.D.; Yao, T.D.; Gao, Y.; Thompson, L.; Mosley-Thompson, E.; Muhammad, S.; Zong, J.B.; Wang, C.; Jin, S.Q.; Li, Z.G. Two glaciers collapse in western Tibet. *J. Glaciol.* **2017**, *63*, 194–197. [CrossRef]
35. Gilbert, A.; Leinss, S.; Kargel, J.; Kääb, A.; Gascoin, S.; Leonard, G.; Berthier, E.; Karki, A.; Yao, T. Mechanisms leading to the 2016 giant twin glacier collapses, Aru Range, Tibet. *Cryosphere* **2018**, *12*, 2883–2900. [CrossRef]
36. Kääb, A.; Leinss, S.; Gilbert, A.; Buhler, Y.; Gascoin, S.; Evans, S.G.; Bartelt, P.; Berthier, E.; Brun, F.; Chao, W.A.; et al. Massive collapse of two glaciers in western Tibet in 2016 after surge-like instability. *Nat. Geosci.* **2018**, *11*, 114–120. [CrossRef]
37. Khromovskih, V.S. *Stone Dragon*; Idea: Moscow, Russia, 1984; 156p. (In Russian)
38. Butvilovsky, V.V. *Paleogeography of the Last Glaciation and the Holocene of Altai: A Catastrophic Events Model*; Tomsk University Press: Tomsk, Russia, 1993; 253p. (In Russian)
39. Rogozhin, E.A.; Platonova, S.G. *Strong Earthquake Source Zones of Gorny Altai in the Holocene*; UIPE RAS: Moscow, Russia, 2002; 130p. (In Russian)